

## Molecular landscape of copy number alterations and genetic mutations in high-grade serous adenocarcinoma of the ovary

Tomoyuki FUKAGAWA<sup>1),2)</sup>, Tamotsu SUGAI<sup>1)</sup>, Wataru HABANO<sup>3)</sup>,  
Makoto EIZUKA<sup>1)</sup>, Noriyuki UESUGI<sup>1)</sup>, Mitsumasa OSAKABE<sup>1)</sup>, Yasuko SUGA<sup>2)</sup>,  
Takayuki NAGASAWA<sup>2)</sup>, Hiroaki ITAMOCHI<sup>2)</sup> and Toru SUGIYAMA<sup>2)</sup>

<sup>1)</sup>Department of Molecular Diagnostic Pathology, School of Medicine,  
Iwate Medical University, Morioka, Japan

<sup>2)</sup>Department of Obstetrics and Gynecology, School of Medicine,  
Iwate Medical University, Morioka, Japan

<sup>3)</sup>Department of Pharmacodynamics and Molecular Genetics, School of Pharmacy,  
Iwate Medical University, Yahaba, Japan

*(Received on January 19, 2018 & Accepted on February 14, 2018)*

### Abstract

Ovarian cancer (OC) is the leading cause of cancer-related death for gynecological cancers. In particular, high-grade serous adenocarcinoma (HGSA) is the most common and aggressive type of OC. Although HGSA exhibits complex genetic alterations, including copy number alterations (CNAs), the molecular mechanisms of HGSA pathogenesis are not fully understood. Single-nucleotide polymorphisms were used to examine genome-wide alterations in ovarian HGSA. In addition, mutations in *TP53*, *KRAS*, *BRAF*, and *PIK3CA* were examined. The highest frequencies of gains in HGSA were found at 8q21-24.3, 3q25.2-27.2, 1q43, and 20q13.33. The most frequent LOHs in HGSA were at 5q12.1-13.3, 4q22.2-24, 8p21.3-22, 16q22.2-23.1, and 22q13.31. In addition, regions of copy-neutral (CN)-LOHs (CN-LOH) in HGSA were detected at 17q21-25 and 17q11-13. The total lengths of the CN-LOHs were significantly

greater in HGSA with lymph node metastasis than in that without lymph node metastasis. Although mutations in *TP53* were frequent, mutations in *KRAS*, *BRAF*, and *PIK3CA* were rarely found in the HGSA specimens examined. The total lengths of the gains were significantly greater in HGSA with *TP53* mutation than in that without *TP53* mutation. Additionally, concurrent *TP53* mutation and CN-LOH at 17p13.1 were frequently found in HGSA. Significant differences in gains between lymph node-positive and -negative samples were observed at 6q16.2-16.3, 6q22.31, and 16q13.2. Furthermore, there were significant differences in the regions of CN-LOH at 9p21-23. These findings suggest the usefulness of genome-wide alterations for the detection of novel frequent genetic alterations that may contribute to HGSA onset or progression.

**Key words** : copy-neutral loss of heterozygosity, copy number alteration, gain, high-grade serous cancer, loss of heterozygosity

Corresponding author: Tamotsu Sugai,  
sugai@iwate-med.ac.jp

### I. Introduction

Ovarian cancer (OC) is the fourth leading cause of cancer-related death in women in

the developed world<sup>1)</sup>. Although various types of cancers have been found in the ovaries, epithelial cancer is the most common type. Epithelial OC can be classified into 4 types, including serous adenocarcinoma (SA), mucinous adenocarcinoma, endometrioid adenocarcinoma, and clear cell carcinoma 2, 3). Serous epithelial ovarian cancer is the most common type, accounting for approximately two-thirds of cases<sup>2, 3)</sup>. Additionally, SA can be further classified into 2 categories (low- and high-grade) based on histological features and tumor grade. High-grade SA (HGSA) is more common than low-grade SA<sup>2, 3)</sup>. HGSA is characterized by high-grade atypia, highly aggressive behavior, and poor prognosis; however, tumors are often sensitive to chemotherapy<sup>2-5)</sup>. Investigation of the biological characteristics of such tumors may provide important insights into the development of next-generation technologies for diagnosis and treatment.

Genomic instability (similar to chromosomal instability) is a hallmark of malignant tumors and is associated with impaired integrity of the genome<sup>6-8)</sup>. As a consequence, numerous genetic alterations and structural changes occur in tumor cells<sup>6-8)</sup>. When genomic instabilities occur repeatedly in tumor cells, the cells acquire growth advantages, suggesting that genomic instability may confer invasive ability on tumor cells<sup>6-8)</sup>. Recent studies have shown that genomic instability is closely associated with carcinogenesis in HGSA<sup>6-8)</sup>. Despite considerable efforts aimed at elucidating the molecular mechanisms of ovarian HGSA, many details of the pathogenesis of HGSA remain unknown. Mutations in *KRAS*, *BRAF*, and *PIK3CA* are rarely found in HGSA<sup>2, 3)</sup>. In contrast,

*TP53* mutations occur in 80% of HGSA, and numerous chromosomal aberrations have been described in HGSA<sup>2-5)</sup>. The recent recognition of HGSA suggests that mutations in *TP53* and chromosomal instability are important molecular events in the pathogenesis of HGSA<sup>9, 10)</sup>.

Genome-wide analysis of DNA copy number alterations (CNAs) has demonstrated the presence of many gains and losses<sup>1, 6, 7)</sup>. These alterations are thought to reflect chromosomal instability in tumor samples<sup>1, 6, 7)</sup>. The aim of the present study was to evaluate the molecular genetic data of this aggressive tumor to determine whether CNAs characterized a subset of HGSA and whether CNAs were associated with *TP53* mutations in HGSA. In addition, we examined whether the extent of CNAs was correlated with clinicopathological parameters, particularly lymph node status.

## II. Materials and Methods

### 1. Patients

The tissue specimens evaluated in this study included 30 cases of invasive HGSA obtained from Iwate Medical University. Histological diagnosis and grading was performed as previously described<sup>11)</sup>. In addition, histological diagnosis was made by expert pathologists (T.S., N.U., and M.O.) after microscopic review of hematoxylin and eosin (HE)-stained slides derived from surgical specimens. Microscopically, HGSA showed papillary and solid growth with slit-like glandular lumens. The tumor cells were typically of intermediate size, with atypical large nuclei and occasional bizarre mononuclear giant cells exhibiting prominent nucleoli. Disease stage was determined using the TNM classification

of the Union for International Cancer Control (UICC)<sup>12)</sup>. The clinicopathological factors examined in this study included age, sex, location, differentiation, lymph node status, and tumor stage.

Patient consent was obtained, and the study was approved by the Iwate Medical University Institutional Review Board.

## 2. Crypt isolation method

Fresh tumor specimens were obtained from resected ovarian cancers.

Isolation of tumor glands was performed as previously described<sup>13, 14)</sup>. Briefly, fresh tumor samples were minced with a razor into small pieces and then incubated at 37°C for 30 min in calcium- and magnesium-free Hanks' balanced salt solution (CMF) containing 30 mM ethylenediaminetetraacetic acid (EDTA). The isolated glands were immediately fixed in 70% ethanol and stored at 4°C.

The fixed isolated glands were observed under a dissecting microscope (SZ 60; Olympus, Tokyo) and were processed routinely to confirm their features using paraffin-embedded histological sections. Contamination by other materials, such as interstitial cells, was not evident in the samples examined in this study.

## 3. DNA extraction

DNA from tumor crypts was extracted by standard SDS proteinase K treatment. DNA extracted from the samples was resuspended in TE buffer (10 mM Tris-HCl, 1 mM EDTA [pH 8.0]) to the equivalent of 1000 cells/ $\mu$ L.

## 4. Analysis of mutations in the *PIK3CA* and *TP53* genes

Single-strand conformation polymorphism (SSCP) analysis was performed as previously described, with some modifications<sup>14, 15)</sup>.

Table 1. Clinicopathological findings of the adnexal high-grade serous adenocarcinoma

	No. of cases	
Total		30
Age (range)	59.5 (31-79)	
median	60	
Location	ovary	27 (90%)
	fallopian tube	3 (10%)
pTNM stage	I-II	9 (30.0%)
	III-IV	21 (70.0%)
Lymph node metastasis	N0	12 (40.0%)
	N1	7 (23.%)
	NX	11 (36.7%)
Pathological grade	1	0
	2	4 (13.3%)
	3	26 (86.7%)

HGSA, high grade serous adenocarcinoma; N0, no regional lymph node metastasis; N1, regional lymph node metastasis; NX, regional lymph nodes cannot be assessed.

Briefly, the polymerase chain reaction (PCR) products (2  $\mu$ L) were mixed with 10  $\mu$ L of gel loading solution, denatured at 95 °C for 5 min, and then kept on ice until loading. Nondenaturing 7.5% polyacrylamide gels were used for electrophoresis (Resolmax; ATTO Co., Tokyo, Japan). The gels were visualized by silver staining and photographed.

Sequencing was performed on the original PCR products of exon 1 of the *PICK3CA* gene and exons 5–8 of the *TP53* gene for all SSCP-positive samples. PCR products were recovered from 3% agarose gels by electrophoresis. Direct sequencing was performed using fluorescently labeled dideoxynucleotide triphosphates for automated DNA sequence analysis (Applied Biosystems 373A sequencer; Applied Biosystems, CA, USA).

## 5. Analysis of *KRAS* and *BRAF* mutations

Mutations in *KRAS* and *BRAF* genes were examined using a pyrosequencer (Pyromark

Q24; Qiagen, NV, USA), as previously described<sup>16</sup>. Samples were amplified by PCR using a *KRAS* v2.0 kit (Qiagen) according to the manufacturer's protocols, as previously described<sup>16</sup>. The purified biotinylated PCR product was set into PyroMark Q24 (Biotage, SE) with PyroMark Gold reagents (Qiagen) containing 0.3  $\mu$ M sequencing primer and annealing buffer.

#### 6. Single nucleotide polymorphism (SNP) array analysis

Total genome copy number alteration (CNA) analysis was performed using an SNP array, as previously described<sup>14, 17</sup>. CNA analysis was performed using an Illumina HumanCytoSNP-12 BeadChip (Illumina, Inc. San Diego, CA, USA) with 299,140 SNP loci, according to the Illumina Infinium HD assay protocol. In the analysis of CNAs, the CNA value was calculated from the B allele frequency (BAF) and log R ratio (LRR) using the Illumina KaryoStudio software program (Plugin v3.0.7.0; Illumina), and chromosomal CNAs were classified as described below. The CNAs were classified using CNA partition algorithms. An LRR of 0 indicated a normal diploid region; an LRR of greater than 0 indicated a copy number gain; and an LRR of less than 0 indicated a copy number LOH. BAF values range from 0 to 1; homozygous SNPs had BAFs near 0 (A-allele) or 1 (B-allele), whereas heterozygous diploid region SNPs had BAFs near 0.5 (AB genotype). Additionally, LRR and BAF data were used to identify regions of hemizyosity and copy-neutral LOH.

To determine the overall chromosomal disruption in HGSA, we developed the chromosomal disruption index (CDI), which

was defined as the total length of CNAs occurring within each chromosomal locus (18). The calculation method is shown below.

#### 7. Calculation of the length of CNAs on a genome-wide scale in HGSA

To quantify CNAs on a genome-wide scale, the total lengths of CNAs (losses + gains), total length of CNA gains, total length of CNA LOHs, and total length of CNA copy-neutral LOHs identified by the SNP-array analysis were calculated (CDI) as previously described. We used the total CNA length as an index representing the degree of chromosomal aberrations and assessed the relationship between CNA length (total CNA, CNA gain, CNA LOH, and CNA copy-neutral LOH) and HGSA.

#### 8. Statistical analysis

Differences in *TP53* mutation distributions between the 2 groups (*TP53* mutation positive and *TP53* mutation negative) were analyzed using Mann-Whitney U tests (PRISM6; GraphPad software, La Jolla, CA, USA). For statistical analysis of differences in lymph node metastasis among the 3 groups (N0, no regional lymph node metastasis; N1, regional lymph node metastasis; NX, regional lymph nodes cannot be assessed), Bonferroni corrections were performed. Differences with p values of less than 0.05 were considered significant.

### III. Results

#### 1. Mutations in the *TP53*, *PIK3CA*, *KRAS*, and *BRAF* genes

All mutant bands detected by SSCP were sequenced and found to contain mutations. Mutations in *TP53* were found in 66.7% (20/30) of carcinomas. The distributions of these mutations were as follows: 20% (4/20) in exon

Table 2. Mutation analysis of the adnexal high-grade serous adenocarcinoma

	No. of cases
Total	30
Mutation	
<i>TP53</i>	20 (66.7%)
<i>PIK3CA</i>	1 (3.3%)
<i>KRAS</i>	2 (6.7%)
<i>BRAF</i>	0

HGSA, high grade serous adenocarcinoma; N0, no regional lymph node metastasis; N1, regional lymph node metastasis; NX, regional lymph nodes cannot be assessed.

5, 10% (2/20) in exon 6, 40% (8/20) in exon 7, and 30% (6/20) in exon 8. A base insertion was found in 1 case (exon 6) and resulted in a stop codon (codon 212–213: TTTCGA-TTTTCGA, T was inserted).

Among the 19 base substitutions, C to T

transversions and G to A transitions were most commonly observed (10 cases, 50%). Other types of mutations were subclassified as G to C (1/20), A to G (2/20), G to T (4/20), C to A (1 of 20), and C to G (1/20). Furthermore, the frequencies of missense and nonsense mutations were 95% (19/20) and 5% (1/20), respectively.

Only one mutation in the *PIK3CA* gene (codon 1025, C to T transversion; 1/30, 3.3%) was detected in the HGSA samples examined. Although no *BRAF* mutations were detected in the HGSA examined in this study, 2 mutations in *KRAS* (G to A transitions, 1/30, 3.3%; G to C transition, 1/30, 3.3%) were found.

## 2. Genomic alterations in HGSA (Table 2)

Chromosomal CNAs were observed in all 30 HGSA. The average frequencies of CNAs across the entire genome are shown in Figure

Table 3. Frequent regions of copy number alterations in high-grade serous adenocarcinoma

a		b		c	
Gain		LOH		CN-LOH	
Chromosomal loci	frequency (%)	Chromosomal loci	frequency (%)	Chromosomal loci	frequency (%)
8q23.3	86.7	5q13.1-13.2	50.0	17q25.1-25.2	83.3
8q24.22	80.0	4q22.3-24	46.7	17q25.3	80.0
8q24.13	76.7	5q12.3	46.7	17q24.3	80.0
8q23.2	76.7	4q22.2	43.3	17q24.2	76.7
3q26.2	73.3	5q13.3	43.3	17q21.33-22	76.7
8q24.21	73.3	5q12.1-12.2	43.3	17q23.1-24.1	73.3
3q26.31-26.32	70.0	8p21.3-22	43.3	17q21.32	70.0
3q26.1	70.0	11p15.4	43.3	17q21.31	60.0
8q24.3	70.0	16q22.2-23.1	43.3	17q12-21.2	56.7
8q24.23	70.0	22q13.31	43.3	17p13.1-13.3	53.3
8q24.11-24.12	70.0			17q11.2	50.0
3q25.33	66.7			17p12	50.0
8q23.1	66.7				
8q22.1	66.7				
1q43	63.3				
3q26.33-27.2	63.3				
3q25.2-25.32	63.3				
8q21.11	63.3				
20q13.33	63.3				

LOH, loss of heterozygosity; CNLOH, copy neutral loss of heterozygosity.

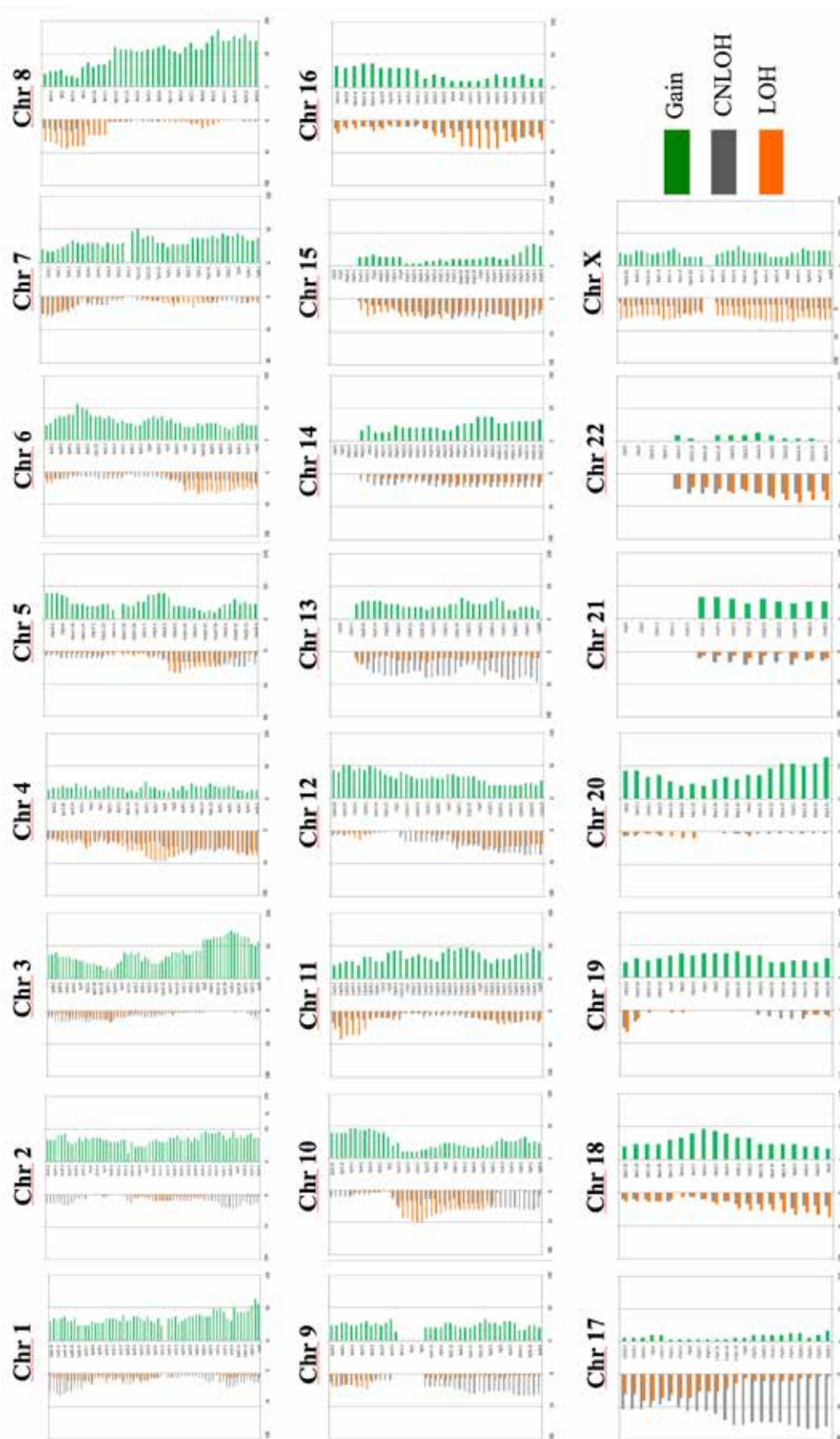


Fig. 1. Ideogram of genomic imbalances in 30 high-grade serous adenocarcinomas. Chromosomes are ordered from 1 to 22. The colored horizontal lines represent the frequencies of gains, LOHs, and copy-neutral LOHs. Lines on the left indicate losses (red, LOHs; gray, copy-neutral LOHs), and those on the right (green) indicate gains.

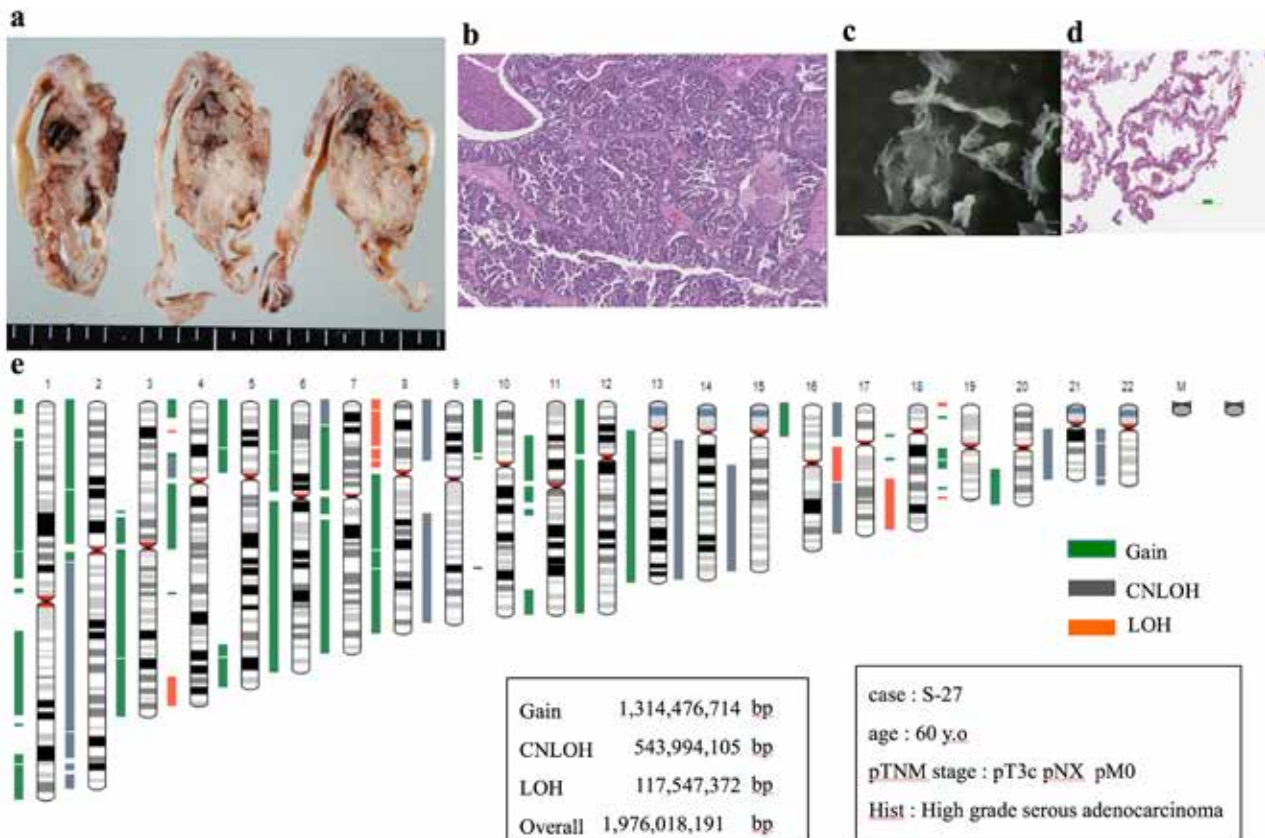


Fig. 2. Representative images of high-grade serous adenocarcinoma. a) Macroscopic features of ovarian serous cancer. b) Low-power view of a lesion showing high-grade serous adenocarcinoma. c) An isolated tumor gland under a dissection microscope. d) High-power histological view of the isolated gland. e) Ideogram showing copy number alterations. Green, gains; red, LOHs; gray, copy-neutral LOHs.

1. The mean total number of chromosomal aberrations per patient was 450, with an average of 210 gains (range: 63–424); the mean number of LOHs was 118 (range: 0–254), and the mean number of copy-neutral LOHs was 122 (range: 12–451). Regions of gains detected in more than 60% of cases were identified at 8q23.3, 8q24.22, 8q24.13, 8q23.2, 3q26.2, 8q24.21, 3q26.31-26.32, 3q26.1, 8q24.3, 8q24.2, 8q24.11-24.12, 3q25.33, 8q23.1, 8q22.1, 1q43, 3q26.33-27.2, 3q25.2-25.32, 8q21.11, and 20q13.33 (Table 3-a). Regions of LOHs detected in more than 40% of the cases were at 5q13.1-13.2, 4q22.3-24, 5q12.3, 4q22.2, 5q13, 5q12.1-12.2, 8p21.3-22, 11p15.4, 16q22.2-23.1, and 22q13.31 in decreasing order of frequency (Table 3-b). On

the other hand, regions of copy-neutral LOHs detected in more than 50% of cases were at 17q25.1-25.2, 17q25.3, 17q24.3, 17q24.2, 17q21.33-22, 17q23.1-24.1, 17q21.32, 17q21.31, 17q12-21.2, 17p13.1-13.3, 17q11.2, and 17p12 (Table 3-c). No minimal common region was detected in the HGSA, given that the alterations were found throughout the entire region.

A representative result for HGSA is shown in Figure 2.

### 3. Relationship between *TP53* mutations and CNAs located at 17p13.1 in HGSA

Concurrent *TP53* mutation and LOH at 17p13.1 were observed in 10 of 20 cases (50%). Additionally, concurrent *TP53* mutation and copy-neutral LOH at 17p13.1 were observed in

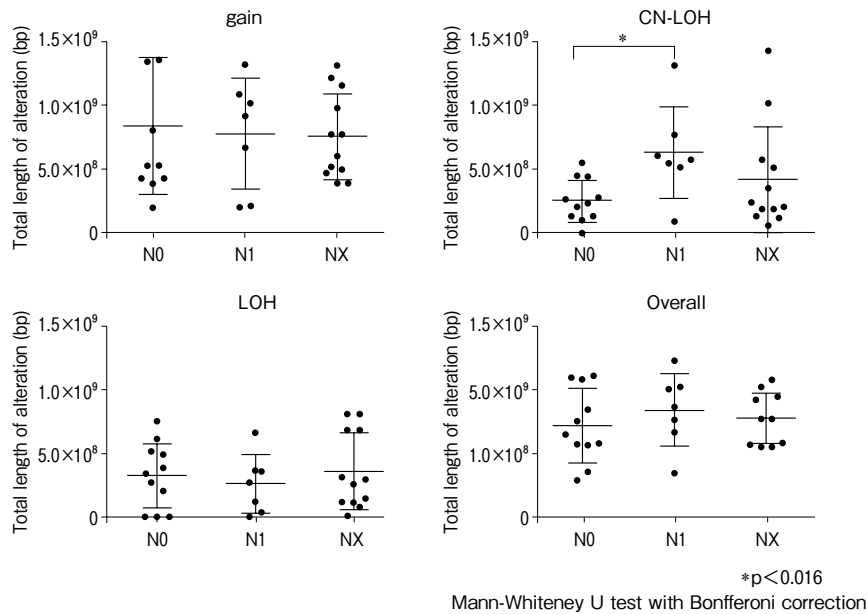


Fig. 3. Comparison of the total lengths of abnormal regions containing CNAs among patients without lymph node metastasis, patients with lymph node metastasis, and patients for whom lymph nodes were not sampled.

Table 4. Comparison of copy number alterations between lymph node positive and negative groups

Gain				CN-LOH			
Chromosomal loci	N0 frequency (%)	N0 frequency (%)	P-value	Chromosomal loci	N0 frequency (%)	N0 frequency (%)	P-value
6q16.3	7.7	7.7	0.014	9q22.33	7.7	71.4	0.014
6q16.2	7.7	7.7	0.014	9q22.1	7.7	71.4	0.014
6q22.31	15.4	15.4	0.044	9q21.33	7.7	71.4	0.044
8q11.21	84.6	84.6	0.044	9q22.32	15.4	71.4	0.044
16p13.2	15.4	15.4	0.044	9q22.31	15.4	71.4	0.044
				9q22.2	15.4	71.4	0.044

CNLOH, copy neutral loss of heterozygosity; N0, no regional lymph node metastasis; N1, regional lymph node metastasis

9 of 20 cases (45%). However, concurrent *TP53* mutation and gain at 17p13.1 were observed in only 1 of 20 cases (5%).

#### 4. Association of length of CNAs on a genome-wide scale and lymph node status in HGSAs

No differences in the overall total lengths of CNAs were observed in HGSAs with or without lymph node metastasis. However, the total length of copy-neutral LOH in HGSAs with lymph node metastasis was longer than

that of HGSAs without lymph node metastasis ( $p < 0.05$ ; Figure 3). In addition, no differences in the total length of CN gain and LOH were observed between HGSAs with or without lymph node metastasis.

#### 5. Association of CNAs with lymph node metastasis in HGSAs

Next, we examined CNAs in HGSAs based on lymph node status. Significant differences in the frequencies of gains at 6q16.3, 6q16.2, 6q22.31, 8q11.21 and 16q13.2 were observed for

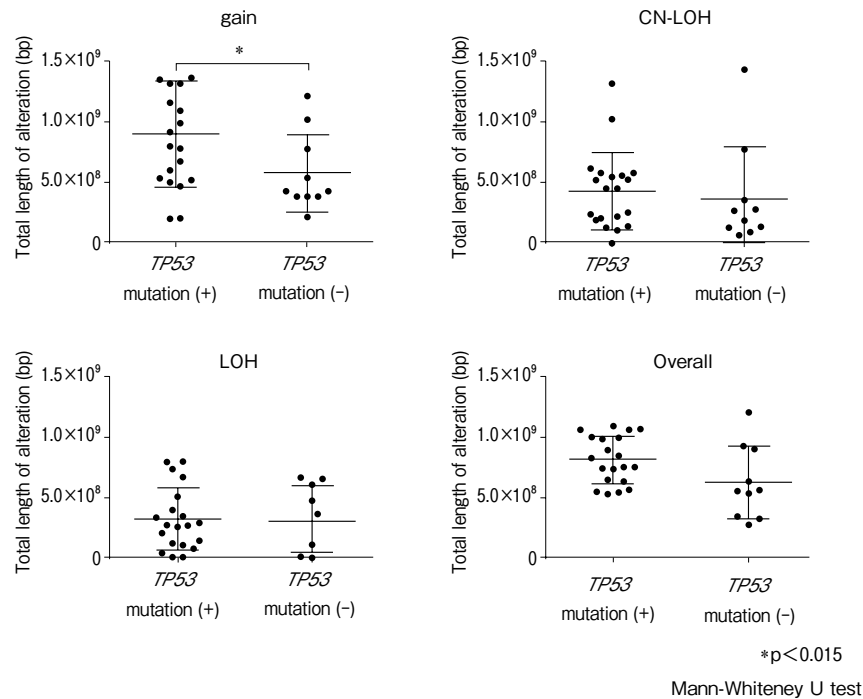


Fig. 4. Comparison of the total lengths of abnormal regions containing CNAs among patients with *TP53* mutations, patients without *TP53* mutations, and patients for whom lymph nodes were not sampled.

HGSAs with positive and negative lymph node metastasis. In addition, significant differences in the frequencies of copy-neutral LOH at 9q22.33, 9q22.1, 9q21.33, 9q22.32, 9q22.31, and 9q22.2 were observed for HGSAs with positive and negative lymph node metastasis. These results are summarized in Table 4.

#### 6. Association of the lengths of CNAs on a genome-wide scale with mutation status of the *TP53* gene in HGSAs

The overall total length of CNAs in HGSAs with *TP53* mutations was longer than that of HGSAs without *TP53* mutations ( $p < 0.05$ ; Figure 4). We analyzed genomic losses (LOHs and copy neutral LOHs) and gains separately. However, there were no significant differences in the total length of CNV gains between HGSAs with *TP53* mutations and HGSAs without *TP53* mutations. Additionally, no significant differences were observed in the

total length of CNV losses between HGSAs with *TP53* mutations and HGSAs without *TP53* mutations.

## IV. Discussion

Genomic CNAs are thought to play a major role in the development and progression of human cancers<sup>1, 6, 7, 19</sup>. Although many CNAs have been reported in ovarian cancers<sup>1, 6, 7, 19</sup>, their genome-wide alterations are not fully understood. Many genetic alterations accumulate during the transition from preneoplastic conditions to the fully malignant phenotype in HGSAs<sup>3-5</sup>. CNAs in cancer cells contribute to the acquisition of invasive ability in tumor cells<sup>1, 16, 17</sup>. In this study, we focused on DNA copy number alterations occurring in HGSAs, as the most common histological type of ovarian cancer.

The identification and targeting of molecular

alterations are impaired by the rich stromal cells that overtake tumor cellularity<sup>13-15)</sup>. Ovarian cancer involves abundant amounts of stromal cells, which are present in the tumor tissue during tumor invasion<sup>20, 21)</sup>. In order to examine genetic alterations in tumor cells, isolation of tumor glands is essential<sup>13-15)</sup>. In the present study, the crypt isolation method was used to enrich the tumor cells in HGSA. This method is easy and inexpensive; thus, it can be used to analyze molecular alterations in tumor cells obtained from routine clinical samples<sup>13-15)</sup>. Additionally, HGSA are known to exhibit tumor heterogeneity in terms of histological feature<sup>2, 3)</sup>. Unfortunately, we could not accurately distinguish the differences in histological appearances of isolated tumor glands under a dissecting microscope. However, we believe that use of isolated tumor glands greatly contributes to accurate evaluation of genetic alterations in HGSA.

The Cancer Genome Atlas (TCGA) is a reliable and widely accepted database; many researchers have used TCGA to evaluate genetic alterations in human cancers, including ovarian cancers<sup>6)</sup>. However, the platform for TCGA was different from that of our study<sup>6, 17)</sup>. Specifically, the differences in the genomic landscapes reflected in the magnitude of gains/losses observed in our results as compared with that in TCGA studies could be a reflection of the methods used for assessment of global genomic abnormalities among the studies<sup>6, 17)</sup>. Thus, data obtained from TCGA cannot be directly compared with our data<sup>17)</sup>. Although frequent copy number gains were common alterations in both data from TCGA and the present study, copy number losses were infrequently observed in

data from TCGA<sup>6)</sup>, in contrast to our result. The difference between the result of TCGA and our result is considered to be one of the reasons that the crypt isolation method was used. Our findings also suggested that both gains and losses play an essential role in the carcinogenesis of HGSA. We believe that our results improve our understanding of the molecular characteristics of HGSA.

Copy number gains are frequently found in various cancers, including ovarian HGSA<sup>6)</sup>, endometrial cancer<sup>22)</sup>, esophageal cancer<sup>23)</sup>, gastric cancer<sup>24)</sup>, and colorectal cancer<sup>25)</sup>. Acquisition of copy number gains is a main driving force for the development and progression of tumors<sup>1, 6, 7)</sup>. Frequent gains at chromosomal loci were observed at 8q21-26, 3p25-26, and 20q13 in the present study. Although gains at 8q24, 8q26, and 3q26 were consistent with data from TCGA<sup>6)</sup>, gains at 8q 21, 8q22, 8q23, 8q25, 3p25, and 20q13, which showed low frequencies in TCGA<sup>6)</sup>, were identified in our results. Thus, our findings suggested that gains at 8q21-26, 1p43, 3p25-26, and 20q13 may be closely associated with the progression of HGSA.

Previous studies have shown that tumor progression is characterized by frequent copy number losses in human cancers<sup>1, 6, 26)</sup>. LOHs occurring in tumor cells are important molecular alterations that play essential roles in colorectal carcinogenesis according to the oncogenic model established by Vogelstein et al<sup>27)</sup>. In our recent studies, however, LOH was found to be an infrequent genetic event in gastric cancer<sup>17)</sup> and colorectal cancer<sup>28)</sup>. Moreover, the current results suggested that ovarian HGSA may be characterized by a high frequency of LOHs. Wang et al.

examined LOH profiles in HGSA using LOH-based clustering analysis and correlated their findings with clinical outcomes in HGSA<sup>29</sup>. Their results showed that HGSA could be separated by LOH-based clustering into characteristic subgroups in 3 different cohorts<sup>29</sup>. In addition, patients in the various LOH clusters differed with respect to chemotherapy resistance, and the extent of LOH was associated with progression-free survival<sup>29</sup>. Thus, we suggest that the LOH pattern defined by genome-wide CNAs may represent a novel clinicopathological parameter for evaluating the molecular mechanisms of ovarian HGSA.

Copy-neutral LOH, defined as acquired uniparental disomy, is a type of copy number loss that is an important genetic event in human cancers<sup>30</sup>. Copy-neutral LOH has been frequently reported in specific types of leukemia<sup>30</sup>. However, recent studies have shown that copy-neutral LOH is also associated with the development of solid type tumors<sup>26, 30</sup>. In the present study, copy-neutral LOH was frequently found in HGSA. To the best of our knowledge, high frequency copy-neutral LOH has not been reported in ovarian HGSA. Although the role of copy-neutral LOH is not fully understood in human cancers, researchers have proposed a link between genomic mutations and copy-neutral LOH, suggesting that mutations, including insertions, deletion, and point mutations, destabilize the DNA structure/function in such a way that copy-neutral LOH is directly promoted during mitotic recombination<sup>30</sup>. According to this model, combination of copy-neutral LOH with mutations may enhance genomic instability, leading to increasing instability at the chromosomal level (chromosomal instability)

in tumor cells<sup>26, 30</sup>. Thus, our findings further confirm that copy-neutral LOH plays a specific role in the progression of ovarian HGSA.

The high frequency of *TP53* mutations in HGSA has been reported in previous studies<sup>31, 32</sup>, consistent with our current results. This finding suggested that *TP53* mutations play a crucial role in carcinogenesis in HGSA<sup>31, 32</sup>. In the present study, we examined the association between *TP53* mutations and copy-neutral LOH at 17p13.1 in HGSA. According to the 2-hit theory for bi-allelic genetic inactivation of tumor-suppressor genes, the function of the *TP53* gene is suppressed<sup>26</sup>. This mechanism is thought to be true for inactivation of genes, such as tumor-suppressor genes, and *TP53* provides a clear example of gene suppression in human cancers, including ovarian cancer<sup>26</sup>. Copy-neutral LOH may represent a novel mechanism for inactivation of *TP53*<sup>26</sup>. Our findings suggested that concurrent *TP53* mutations and copy-neutral LOH at 17p13.1, as detected in the present study, may enhance the effects of *TP53* mutation within the tumor, thereby disrupting key regulatory pathways linked to the *TP53* signaling pathway<sup>30</sup>. Our results suggested that concurrent mutations and copy-neutral LOH at the corresponding locus may cause enrichment of deleterious mutations in tumor cells in HGSA.

In the present study, the total length of CNAs occurring in all chromosomes was used as the CDI<sup>7, 18</sup>. Lymph node metastasis has not been reported in TCGA data.

The CDI of copy-neutral LOHs was significantly higher in the lymph node metastasis group than in the non-metastasis group. In addition, the CDI (defined as the

level of genomic alterations) of copy number gains in the case of *TP53* mutations, which are associated with invasive ability, was higher than that in cases without *TP53* mutations, supporting the aggressive nature of HGSA. We suggest that this index may be useful to assess the degree of chromosomal alterations and could be used to predict tumor aggressiveness by applying CDI in HGSA.

In the current study, differences in the frequencies of copy-neutral LOHs between HGSA with or without lymph node metastasis were found at 9q21-22. Additionally, 6q16.2-3, 6q22.31, and 16p13.2 were the most common loci at which gains were observed in HGSA with lymph node metastasis. Several candidate genes were identified within these chromosomal loci; however, candidate genes associated with lymph node metastasis have not been identified in ovarian HGSA. Despite this, our results may provide important insights into the roles of chromosomal alterations in the progression of HGSA.

Candidate genes within these loci that are associated with lymph node metastasis should be explored in future studies.

## V. Conclusions

We performed a comprehensive examination of CNAs using isolated tumor glands obtained from ovarian HGSA. Our findings illustrate the unique molecular profile that characterizes the aggressive behavior of HGSA. In addition, candidate chromosomal alterations obtained from our results should be confirmed to determine whether such alterations may be useful as novel molecular markers.

## Acknowledgments

We gratefully acknowledge the technical assistance of Ms. E. Sugawara and Mr. T. Kasai. We also thank members of the Department of Molecular Diagnostic Pathology, Iwate Medical University for their support.

Conflict of interest: The authors have no conflict of interest to declare.

## References

- 1) **Engler DA, Gupta S, Growdon WB, et al.:** Genome wide DNA copy number analysis of serous type ovarian carcinomas identifies genetic markers predictive of clinical outcome. *PLoS One* 7: e30996. doi: 10.1371, 2012.
- 2) **McCluggage WG:** Morphological subtypes of ovarian carcinoma: a review with emphasis on new developments and pathogenesis. *Pathology* 43, 420-432, 2011.
- 3) **Kurman RJ and Shih IeM:** The origin and pathogenesis of epithelial ovarian cancer: a proposed unifying theory. *Am J Surg Pathol* 34, 433-443, 2010.
- 4) **Prat J:** New insights into ovarian cancer pathology. *Ann Oncol* 23 (Suppl 10), x111-117, 2012
- 5) **Prat J:** Pathology of cancers of the female genital tract. *Int J Gynaecol* 131 (Suppl 2), S132-145, 2015.
- 6) Cancer Genome Atlas Research Network: Integrated genomic analyses of ovarian carcinoma. *Nature* 474, 609-615, 2011.
- 7) **Cope L, Wu RC, Shih IeM, et al.:** High level of chromosomal aberration in ovarian cancer genome correlates with poor clinical outcome. *Gynecol Oncol* 128, 500-505, 2013.
- 8) **Martin SA, Hewish M, Lord CJ, et al.:** Genomic instability and the selection of treatments for cancer. *J Pathol* 220, 281-289, 2010.
- 9) **Capo-chichi CD, Cai KQ, Simpkins F, et al.:** Nuclear envelope structural defects cause chromosomal numerical instability and aneuploidy in ovarian cancer. *BMC Med* 9:28. doi: 10.1186/1741-7015-9-28, 2011.
- 10) **Svobodova K, Zemanova Z, Lhotska H, et al.:** Copy number neutral loss of heterozygosity at 17p and homozygous mutations of TP53 are

- associated with complex chromosomal aberrations in patients newly diagnosed with myelodysplastic syndromes. *Leuk Res* **42**, 7-12, 2016.
- 11) Japanese Society of Obstetrics and Gynecology: The general rules for clinical and pathological management of ovarian tumors part 1: histological classification and color atlas of ovarian tumors, 2nd ed. pp.1-41, Kanehara, Tokyo, 2009.
  - 12) **Wittekind C, Gospodarowicz MK and Sobin LH**: Union for international cancer control UICC TNM classification of malignant tumours, 7th ed. Wiley-Blackwell, New Jersey, 2009.
  - 13) **Habano W, Sugai T, Yoshida T, et al.**: A novel method for gene analysis of colorectal carcinomas using a crypt isolation technique. *Lab Invest* **4**, 933-940, 1996.
  - 14) **Suga Y, Sugai T, Fukagawa T, et al.**: Molecular analysis of isolated tumor glands from endometrial endometrioid adenocarcinomas. *Pathol Int* **65**, 240-249, 2015.
  - 15) **Sugai T, Habano W, Sasou S, et al.**: Use of crypt isolation to determine loss of heterozygosity of multiple tumor suppressor genes in colorectal carcinoma. *Pathol Res Pract* **196**, 145-150, 2000.
  - 16) **Yamamoto E, Suzuki H, Kamimae S, et al.**: Molecular dissection of premalignant colorectal lesions reveals early onset of the CpG island methylator phenotype. *Am J Pathol* **181**, 1847-1861, 2012.
  - 17) **Arakawa N, Sugai T, Sugimoto R, et al.**: Genome-wide analysis of DNA copy number alterations in early and advanced gastric cancers. *Mol Carcinog*, doi: 10.1002, 2016.
  - 18) **Sawada T, Yamamoto E, Suzuki H, et al.**: Association between genomic alterations and metastatic behavior of colorectal cancer identified by array-based comparative genomic hybridization. *Genes Chromosomes Cancer* **52**, 140-149, 2013.
  - 19) **Baumbusch LO, Helland Å, Wang Y, et al.**: High levels of genomic aberrations in serous ovarian cancers are associated with better survival. *PLoS One* **8**:e54356, doi: 10.1371/journal.pone.0054356, 2013.
  - 20) **Yang Z, Xu S, Jin P, et al.**: MARCKS contributes to stromal cancer-associated fibroblast activation and facilitates ovarian cancer metastasis. *Oncotarget* **7**, 37649-37663, 2016.
  - 21) **Corvigno S, Wisman GB, Mezheyski A, et al.**: Markers of fibroblast-rich tumor stroma and perivascular cells in serous ovarian cancer: Inter- and intra-patient heterogeneity and impact on survival. *Oncotarget* **7**, 18573-18584, 2016.
  - 22) Cancer Genome Atlas Research Network: Integrated genomic characterization of endometrial carcinoma. *Nature* **497**, 67-73, 2013.
  - 23) Cancer Genome Atlas Research Network: Genetic landscape of esophageal squamous cell carcinoma. *Nat Genet* **46**, 1097-1102, 2014.
  - 24) Cancer Genome Atlas Research Network: Comprehensive molecular characterization of gastric adenocarcinoma. *Nature* **513**, 202-209, 2014.
  - 25) Cancer Genome Atlas Network: Comprehensive molecular characterization of human colon and rectal cancer. *Nature* **487**, 330-337, 2012.
  - 26) **Ryland GL, Doyle MA, Goode D, et al.**: Loss of heterozygosity: what is it good for? *BMC med genomics*, doi: 10.1186/s12920-015-0123-z, 2015.
  - 27) **Vogelstein B, Fearon ER, Hamilton SR, et al.**: Genetic alterations during colorectal tumor development. *N Eng J Med* **319**, 525-532, 1988.
  - 28) **Takahashi Y, Sugai T, Otsuka K, et al.**: Molecular differences in the microsatellite stable phenotype between left-sided and right-sided colorectal cancer. *Int J Cancer* **139**, 2493-2501, 2016.
  - 29) **Wang ZC, Birkbak NJ, Culhane AC, et al.**: Profiles of genomic instability in high-grade serous ovarian cancer predict treatment outcome. *Clin Cancer Res* **18**, 5806-5815, 2012.
  - 30) **Stirewalt DL, Pogossova-Agadjanyan EL, Tsuchiya K, et al.**: Copy-neutral loss of heterozygosity is prevalent and a late event in the pathogenesis of FLT3/ITD AML. *Blood Cancer J* e208, doi: 10.1038/bcj.2014.27, 2014.
  - 31) **Wojnarowicz PM, Oros KK, Quinn MC, et al.**: The genomic landscape of TP53 and p53 annotated high grade ovarian serous carcinomas from a defined founder population associated with patient outcome. *PLoS One*, doi:10.1371/journal.pone.0045484, 2012.
  - 32) **Hunter SM, Anglesio MS, Ryland GL, et al.**: Molecular profiling of low grade serous ovarian tumours identifies novel candidate driver genes. *Oncotarget*, doi: 10.18632/oncotarget.5438, 2015.

## 卵巣高異型度漿液性腺癌における 高密度 SNP array を用いた分子解析

深川智之<sup>1,2)</sup>, 菅井 有<sup>1)</sup>, 幅野 渉<sup>3)</sup>,  
永塚 真<sup>1)</sup>, 上杉憲幸<sup>1)</sup>, 刑部光正<sup>1)</sup>, 菅安寿子<sup>2)</sup>,  
永沢崇幸<sup>2)</sup>, 板持広明<sup>2)</sup>, 杉山 徹<sup>2)</sup>

<sup>1)</sup>岩手医科大学医学部, 病理診断学講座

<sup>2)</sup>岩手医科大学医学部, 産婦人科学講座

<sup>3)</sup>岩手医科大学薬学部, 薬物代謝動態学講座

*(Received on January 19, 2018 & Accepted on February 14, 2018)*

### 要旨

卵巣癌は婦人科癌関連死の主要な原因の一つで, 卵巣癌の中で漿液性腺癌は高頻度かつ予後不良な組織型である. 漿液性腺癌は複雑な遺伝子変化を示すが, 分子発癌機序は完全には明らかにされていない. 一塩基多型を用いて, 漿液性腺癌のゲノムワイドな変化と TP53 等の遺伝子変異と臨床病理学的特徴との関連について検討した. 8q21-24.3 に gain を, 5q12.1-13.3 に loss of heterogeneity (LOH) を, 17q21-25 に Copy-neutral (CN)-LOH を多く検出した. リンパ節転移陽

性群では CN-LOH 領域の総塩基長が有意に長かった. TP53 変異は高頻度であったが, 他の遺伝子変異はほとんど確認されなかった. TP53 変異陽性群では gain 領域の総塩基長が有意に長かった. リンパ節陽性例の gain は 6q16.2-16.3, 6q22.31, 16q1, CN-LOH は 9p21-23 の領域で有意に高頻度であった. これらの知見はゲノムワイドな遺伝子変化を検出することで漿液性腺癌の発症, 進行に関わる新規の遺伝子変化を特定することに寄与する可能性がある.